Journal of GeoEngineering, Vol. 2, No. 3, pp. 123-128, December 2007

Case Record:

FIELD TESTING OF AXIALLY LOADED DRILLED SHAFTS IN CLAY/GRAVEL LAYER

San-Shyan Lin[1], Kun-Jui Wang[2], Hsii-Sheng Hsieh[2], Yu-Herng Chang[3], and Chien-Shun Huang[4]

ABSTRACT

This paper examines six case histories of load tests on reverse circulation method installed drilled shafts, with or without tip grouting, under axial load. Shaft displacement readings based on both telltale/extensometer and rebar gage are compared first. Subsequently, effect of loading cycle on shaft elastic modulus estimation is evaluated. The load versus displacement relationships at shaft head, the t-z curves of clay layer and of gravel layer are other important concerns and are compared in the paper. In addition, the adhesion factor α and the parameter β based on the pile load test results are suggested in the paper.

Key words: Pile load test, drilled shaft, reverse circulation method, tip grouting, case study.

1. INTRODUCTION

In some area of Taipei City, over tens of meters thick of gravelly soil layer sandwiched between top silty clay layer and bottom bedrock can often be found. Increasing use of rock socket drilled shafts in many building projects in Taipei and how to estimate side friction resistance of shaft through gravelly soil layer have been major concerns for local geotechnical engineers. In addition, effect of tip grouting on skin friction resistance through gravelly soil layer is another concern.

Bearing capacity of drilled shafts in gravel formation has drawn geotechnical engineer's attention in the past decade, such as the available researches by O'Neill and Reese (1999) and by Rollins *et al*. (2005). These researchers conducted a series of uplift tests on drilled shaft in soil profiles ranging from uniform sand to sandy gravel to evaluate side friction in gravel soils. These researches were all focused on the gravel layer right under ground surface.

To compare the axial performance of drilled shafts through gravel layer, six instrumented drilled shafts with and without tip grouting installed at eastern Taipei area were selected and evaluated based on pile load test results. Summary of test shaft geometry and measured capacity is given in Table 1. All the shafts were cast-in-place Portland cement concrete piles and were installed by the same contractor. The modified U-shape grouting device (Lin *et al*. 2000) was pre-installed on three pre-selected shafts for tip grouting purpose. Telltale/extensometer and rebar gage were used and installed in the test shaft to obtain information on load transfer in side and tip resistance. The telltales were extended to several selected depths along the length of the shaft to measure the movements of the telltale rods relative to the head of the drilled shaft. The internal load in the shaft was obtained at selected depth by multiplying the axial stiffness of the test shaft (Cross-sectional area at the selected depth times composite modulus of the shaft) by the strain obtained at the depth of interest (O'Neill and Reese 1999). Results based on the instrumented rebar gage can also be obtained by similar procedures.

In the following, measured data obtained from both rebar gage and telltale/extensometer are compared first. Subsequently, effect of loading cycle on elastic modulus estimation is studied. The load versus settlement relationship at head and the t-z curves along shaft are also main concerns and are compared in the paper. Finally, the adhesion factor α and the parameter β based on the pile load test results are also suggested in the paper.

2. SITE LOCATION AND GROUND CONDITIONS

The six shafts were installed at five locations within the test site located in Eastern Taipei, as shown in Fig. 1. In addition to top 3 m of backfill material, typical soil conditions at the site from ground surface down consists of ~50 m of low plasticity clay layer and ~15 m of gravelly soil layer, which contains about 42 to 70 percent gravel, 28 to 42 percent sandy soil and other fine soils. Beneath the gravel layer, sandstone bedrock is encountered. Typical subsurface soil physical and strength properties are presented in Table 2 and Fig. 2. Figure 3 gives the undrained shear strength of the top silt clay layer along depth. Contour lines of the top of gravel layer and bedrock of the site are shown in Figs. 4 and 5, respectively.

3. CONSTRUCTION

The reverse circulation method was used for shaft installation, and drilling was done with polymer slurry pumped into a shaft borehole while the slurry-soil mixture was discharged from the centrally placed air-lift riser pipe to allow settlement in the tank to facilitate the removal of soil particles. All shafts were concreted using tremie method. Four 5.08 cm PVC pipes were attached to the rebar cage of each shaft for sonic logging integrity testing. To evaluate the total load carried at different depths

---

Manuscript received September 28, 2007; accepted November 15, 2007.

[1] Professor, corresponding author, Department of Harbor and River Engineering, National Taiwan Ocean University, Keelung, Taiwan 20224 (e-mail: sslin@mail.ntou.edu.tw).

[2] Engineer, Trinity Foundation Engineering Consultants, Taipei, Taiwan.

[3] Vice President, Diagnostic Engineering Consultants, Ltd., Taipei, Taiwan.

[4] President, Great Asia Engineering Consultants, Taipei, Taiwan.

Table 1 Test shafts geometry and measured capacity

	Diameter (m)	Length (m)	Tested loading (MN)	Side resistance (MN)	Tip resistance (MN)	Head settlement (mm)	Tip settlement (mm)	Loading cycle	Tip grouting (m^3)	Side resistance/Tested load	Tip resistance/Tested load
Case-1	1.2	76.0	36.3	35.9	0.4	70.8	6.8	2-Cycle	–	99%	1%
Case-2	1.5	65.0	37.7	35.8	1.9	33.8	8.7	1-Cycle	2.7	95%	5%
Case-3	1.5	56.0	26.5	22.6	3.9	29.0	9.3	3-Cycle	6.6	85%	15%
Case-4	1.2	59.0	24.5	23.7	0.8	17.4	0.3	5-Cycle	3.2	96%	3%
Case-5	2.5	70.3	55.9	54.8	1.1	17.4	7.0	1-Cycle	–	98%	2%
Case-6	2.0	70.7	39.2	39.2	0.0	17.4	0.0	1-Cycle	–	100%	0%

Table 2 Soil properties of the test site

No.	Soil type	Depth, m	SPT-N	γ_t, kN/m^3	W_n, %	W_L,%	I_p, %	e	E_s, MPa
1	Fill (SF)	0-3	3-50	17.7-18.2 (18.2)	29-36.9 (34.1)			0.89-0.97 (0.93)	
2	Silty clay (CL)	1.7-32.6 (30.5)	2-7 (4)	16.1-18.3 (17.6)	33-41 (35.7)	35-44 (40.7)	14-21 (17.7)	0.99-1.34 (1.07)	16 ~ 56
3, 4 (interstratified layers)	Silty clay or sandly silt (CL-ML, SM)	29.1-53	13-37 (19)	17.7-18.8 (18.5)	24-30 (28)	33-36 (34.5)	13-15 (14)	0.82-0.9 (0.86)	56 ~ 80
	Silty sand with some gravel layer (SM/ML.GW)	30.7-53	10-50	17.9-19.6 (19.1)	20.2-33.6 (24)			0.66-1.2 (0.92)	40 ~ 100
5	Sandly gravel (GM/GW)	49.4-66.6	24-50	18.6-21.6 (19.8)	15-32 (22.6)			0.7-0.9 (0.78)	200
6	Bed rock (SS/SH/MS)	54.6-	> 50	19.6-22.9 (21.9)	11-13 (12)				200

Note: γ_t : total density ; W_n : natural water content ; W_L: liquid limit ; I_P: plasticity index ; e: void ratio ; Es: elastic modulus; ( ) : average

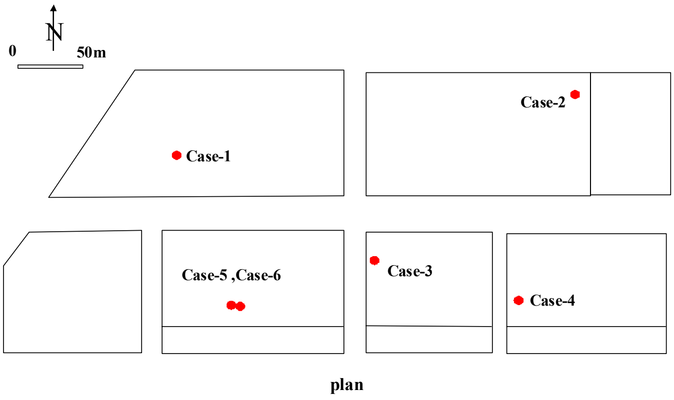

Fig. 1 Site plan and locations of test shafts

along the shaft, both rebar gages and telltale/extensometer were installed at several selected depths of each shaft (Fig. 6). The rebar gages were attached to the rebar cage in sets of four at each depth and were protected.

4. TIP GROUTING

Shafts that were considered for tip grouting, a modified U-shape cleaning/grouting device was pre-installed at the tip of the shaft. A high-pressure water jet was used to clean undesirable material from the shaft base first. After the shaft concrete reached the required strength, high-pressure water was used to force the sediment or weak material below the tip of the shaft off the concrete surface. Using the drilling rig, a drilling rod was lowered through the pre-installed sonic logging tube to the bottom of the shaft. The water was pressurized at between 14.7 and 19.6 MPa. In the mean time, while maintaining a rotation speed of 6 to 8 RPM, the rod was lowered at a speed of 100 mm/min within about 30 cm or deeper of the shaft base. The water circulated at least two times to and through the soft bottom of the shaft.

Subsequently, low-pressure washing at 5 MPa was used to force the solids or debris to the ground surface with returning water. The returning water was monitored until it turned clean. Washing was stopped once the returning water remained clean over a given period of time.

After cleaning of the base sediment was completed, the grout, at a pressure of 2 to 5 MPa, was injected through one of the sonic logging holes. Only two holes were used for grouting each time, the other two holes were packed off. A packer was used to prevent the grout from returning up the injection hole. The grout used was composed of water and cement at a water/cement ratio of 1:1. Once the grout returned from the other grouting hole, the valve was shut; however, injection of grout continued under the same pressure for about five minutes or until a pressure of higher than 4,900 kPa was needed to finish the

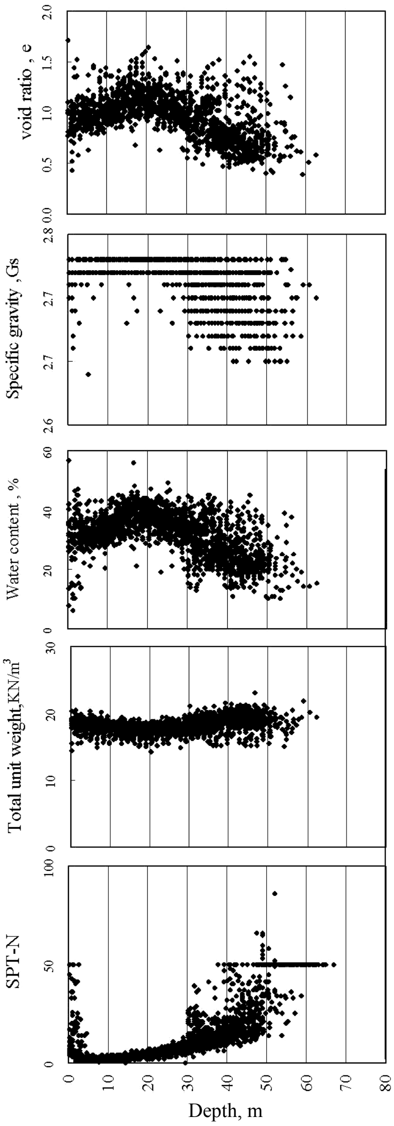

Fig. 2 Soil properties of the test site

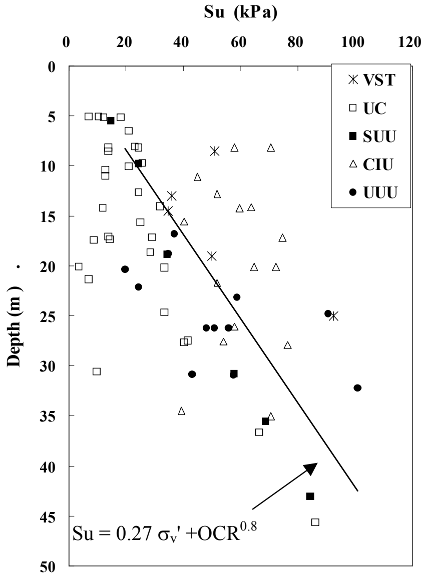

Fig. 3 Undrained shear strength of the top clay layer along depth

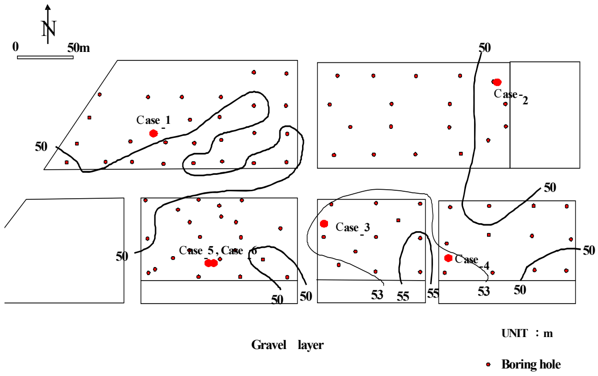

Fig. 4 Contours of the top elevation of the gravelly soil layer

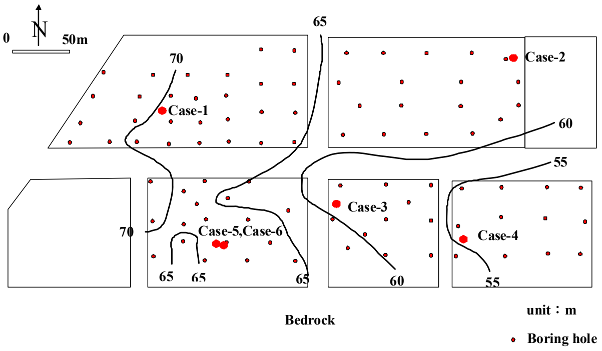

Fig. 5 Contours of the top elevation of the bedrock

grouting process. The 4,900 kPa pressure was set based on the experience of local engineers. In addition, the excess water at the shaft bottom was returned before the grout from the other grouting hole. Detail information of the tip grouted shafts is shown in Table 3.

5. SHAFT LOAD TESTS AND TEST RESULTS

Settlement readings were taken immediately after each load increment and at one minute and then at every two minutes before increasing the load. When the maximum load was reached, the loading was maintained until the settlement rate was less than 0.25 mm/hr before unloading. Then, the maximum loading was unloaded by four decrements.

In order to estimate frictional resistance along the shaft, information of the strain at different depths of the shaft and the modulus of the concrete and the steel is required. The axial load is the strain multiplied by cross sectional area of the pile and the elastic modulus, the following equation is often used

$$P = \varepsilon \cdot (A_c \cdot E_c + A_s \cdot E_s) \quad (1)$$

Where P = axial force of the considered cross section; A_c = cross sectional area of concrete; A_s = cross sectional area of steel; and E_s = elastic modulus of steel. Variation of strain along shaft can be obtained from either telltale/extensometer or rebar gage readings. Depths considered for telltale/extensometer and rebar gage readings of each shaft are shown in Fig. 6. Comparing to the rebar gage, telltale or extensometer is considered to be easier to install and also cheaper. The difference of the readings from telltale/extensometer and rebar gage is given in Fig. 7. Apparently, the readings obtained from either telltale or extensometer is

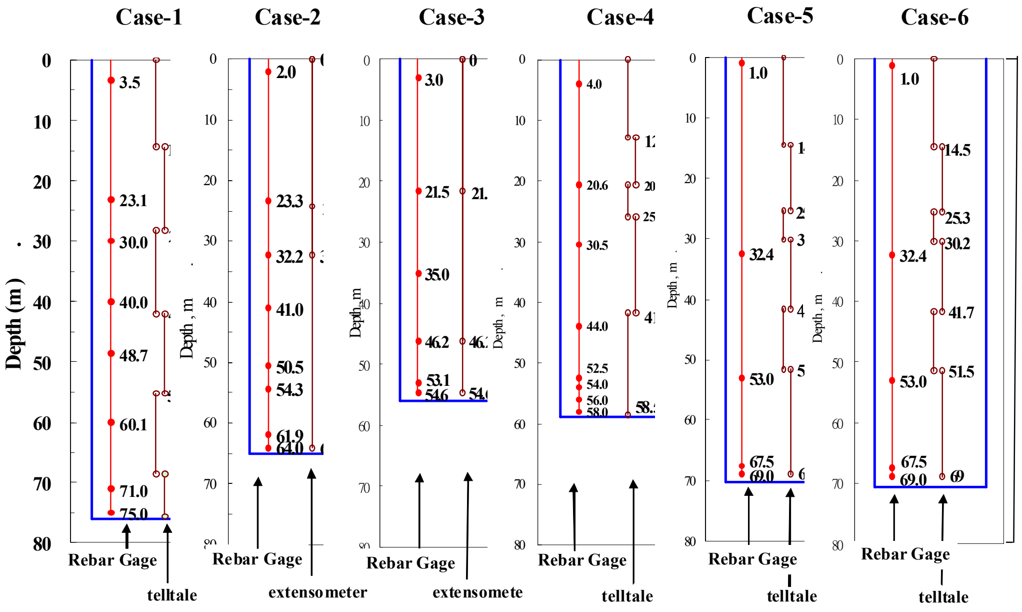

Fig. 6 Selected depths of the telltale/extensometer and rebar gage

Table 3 Quantity of grout used for tip grout of Cases 2 to 4

	Shafts		Tip grouting range		Washing or grouting pressure			Grouting volume	Grout volume / washed volume
	Diameter (m)	Length (m)	Start (m)	End (m)	1st washed (MPa)	2nd washed (MPa)	Grouting (MPa)	(m^3)	
Case-2	1.5	65.0	65.0	65.3	14.7	5.0	2 ~ 5	2.66	1.7
Case-3	1.5	56.0	56.0	59.0	19.6	5.0	2 ~ 5	5.43	0.9
Case-4	1.2	59.0	59.6	60.6	19.6	5.0	2 ~ 5	3.20	1.6

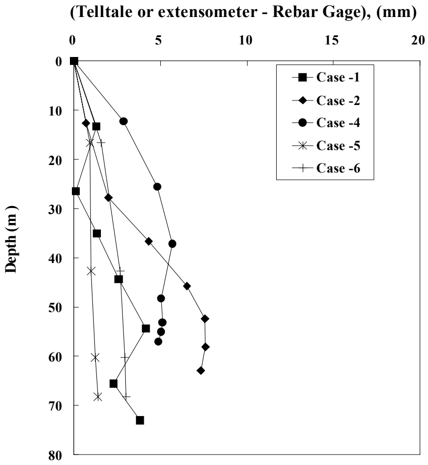

Fig. 7 Difference of readings between telltale/extensometer and rebar gage

higher than that of the rebar gage. None of the available researches discussed which reading data is more accurate. Local engineer's experience believes the data obtained from rebar gage is more reliable and is hence used in the following shaft friction resistance estimation. However, the reason why rebar gage reading is more reliable than that of telltale/extensometer still needs further study.

Strain reading of the rebar gage located nearest to the pile head is often used for concrete modulus estimation; the modulus calculated for each increment affected by shaft resistance is negligible and hence the calculated tangent modulus is close to the actual one, as suggested by Fellenius (2001). In addition, similar to the observation by Fellenius (2001), the modulus values are also strain dependent as shown in Fig. 8 for the studied cases. Further, it is observed in this study that the modulus values are also test loading cycle dependent as shown in Fig. 9. Increasing the number of loading cycle, the modulus value decreases with increasing strain. Selected modulus value versus strain curve for Case 4 is also indicated in Fig. 9. The method for concrete secant modulus determined from tangent modulus suggested by Fellenius (2001) is adopted in this paper.

The normalized t-z curves of the silt clay layer, gravel layer and the bedrock layer are given in Figs. 10 to 13, respectively. Ultimate resistance has been reached at silty clay layer but not for gravel soil and bedrock. Strain softening was also observed for tip grouted cases of 2 to 4 at lower silty clay layer. For gravelly soil layer, the side friction resistance corresponding to the measured displacement of 15 mm is considered as the ultimate value as suggested by Woo (2001).

For the cases without tip grouting, the ultimate skin frictional resistance of silty clay layer versus SPT-N is shown in Fig. 14, in which the f_s = N, 3.3 N, and 5 N are the suggested design code of correlations Canadian and Japanese highways as well as Japanese buildings, respectively. Higher resistance was observed than that of the suggested design code values under lower SPT-N value. The ratios of the ultimate skin frictional resistance to the SPT-N value for the cases with and without tip grouting are shown in Fig. 15. The f/ SPT-N ratio appears to be decreasing with increasing of SPT-N value s. Apparently, the cases with tip grouting also increase their skin friction resistance. For the SPT-N value less than 50, the best fitted results for the cases with and without tip grouting can be expressed as

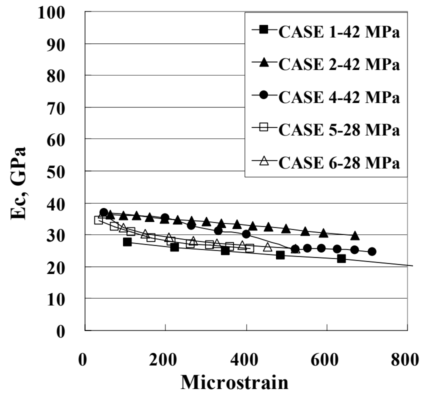

Fig. 8 Concrete modulus versus measured strain

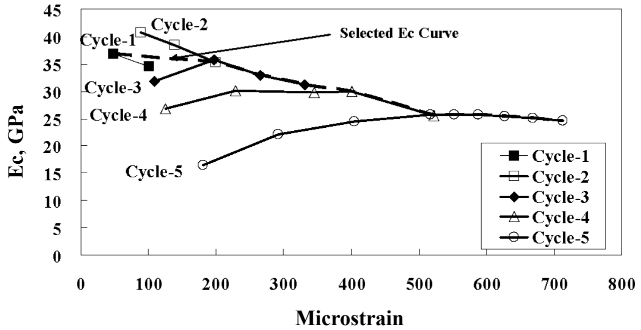

Fig. 9 Effect of loading cycles on concrete modulus

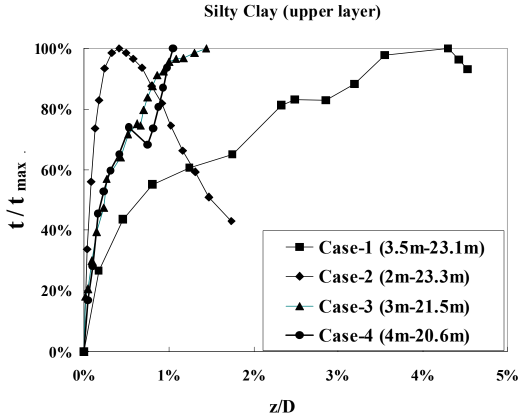

Fig. 10 Normalized t-z curves of the upper silt clay layer

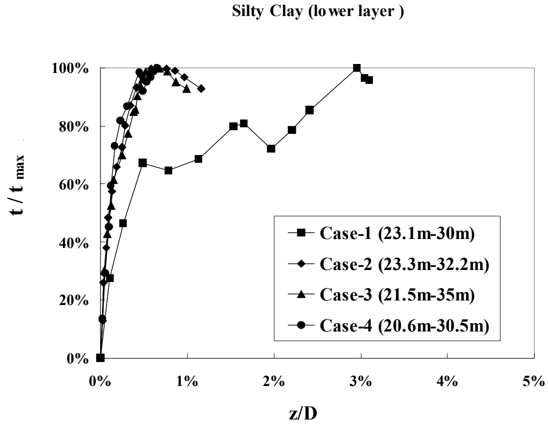

Fig. 11 Normalized t-z curves of the lower silt clay layer

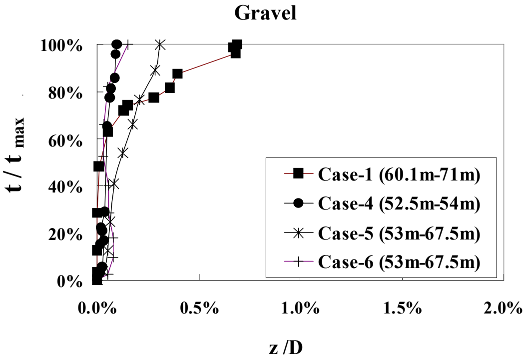

Fig. 12 Normalized t-z curves of the gravelly soil layer

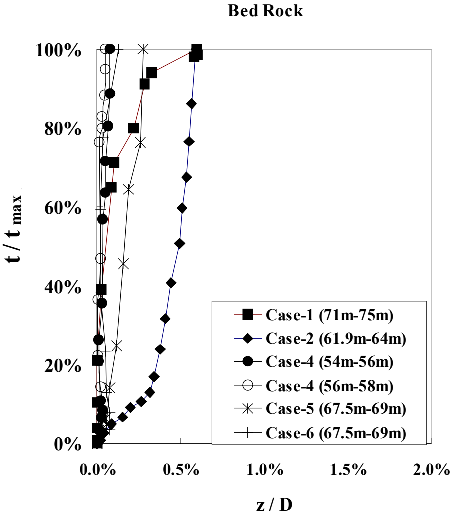

Fig. 13 Normalized t-z curves of the bedrock

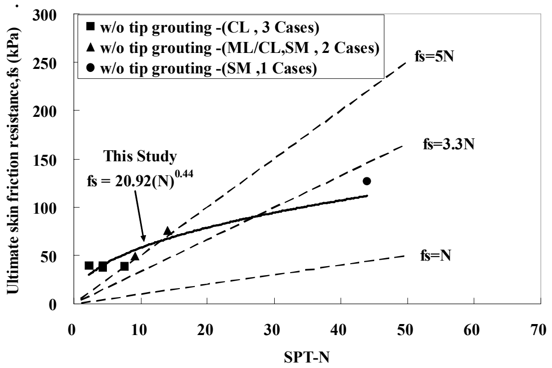

Fig. 14 Relation between ultimate skin frictional resistance versus SPT-N values

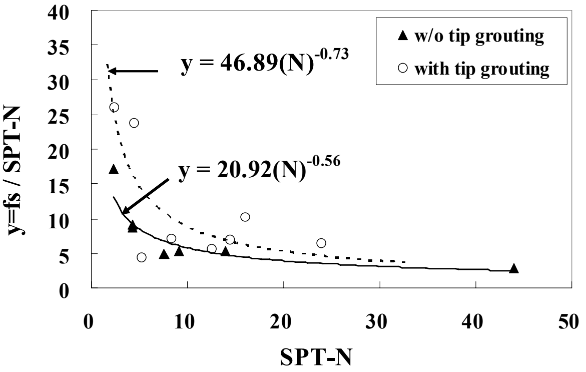

Fig. 15 Relation of f_s / SPT-N versus SPT-N values

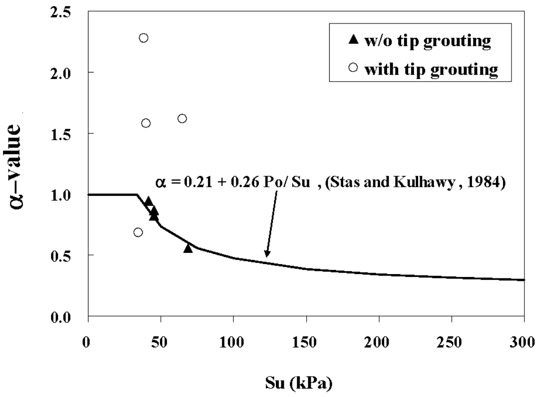

Fig. 16 Back-calculated α-value versus undrained shear strength

$$f_s\,/\,\text{SPT-N} = 46.89(\text{N})^{-0.73} \tag{2}$$

and

$$f_s\,/\,\text{SPT-N} = 20.92(\text{N})^{-0.56}\,, \tag{3}$$

respectively. For the top silt clay layer, the α values obtained from the pile load test results are shown in Fig. 16. For the cases without tip grouting, the α value well fits the α versus undrained strength relationship of the clay as recommended by Stas and Kulhawy (1984). However, three of the four α data for the shafts with tip grouting treatment are significantly higher than the recommendation by Stas and Kulhawy (1984).

The β values along depth from the pile load test results are shown in Fig. 17, in which the recommended values by O'Neill and Reese (1999) and by Rollins *et al.* (2005) are also given for comparison. Since only uplift load tests were conducted by Rollins *et al.* (2005), the modified Rollins *et al.* (2005) curve was modified based on the suggestion by Rollins *et al.* (2005) that the shaft resistance in tension could be 12-25 percent smaller than in compression. 25 m and 35 m are the limit depth of gravel layer considered by O'Neill and Reese (1999) and by Rollins *et al.* (2005), respectively. Based on the above studied cases, suggested design parameters are summarized in Table 4.

6. CONCLUSIONS

Based on the results of the six case histories discussed in this paper, the following conclusions are drawn:

1. In addition to the effects of the measured strain and measured depth, the elastic modulus of the shaft concrete is also affected by the test loading cycles.
2. Side frictional resistance for the clay and the gravel layer are 37 to 39 kPa and 149 to 188 kPa, respectively.
3. Comparison on the shaft test results for the shafts with and without tip grouting show tip grouting improves mainly the shaft frictional resistance.
4. Back-calculated α value of the clay layer is between 0.7 and 0.95.
5. Back-calculated β value of the clay layer and gravel layer is 0.13 to 0.3 and 0.28 to 0.38, respectively.
6. By using SPT-N value for side friction resistance estimation, the ultimate skin resistance is bounded between 3N (kPa) and 5N (kPa).

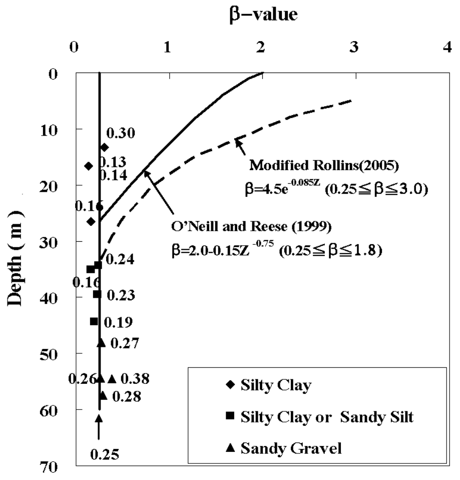

Fig. 17 Variation of β-value with depth

Table 4 Summary of design parameters suggested based the studied cases

Soil type	Ultimate skin resistance, f_s (kPa)	α-method (α-value)	β-method (β-value)	SPT-N method	Z^* (mm)	$z\,/\,D^*$ (%)
Silty clay (CL)	37-39 (38)	0.7-0.95 (0.8)	0.13-0.30 (0.18)	5N-17N	3-22 (11.6)	0.4%-1.4% (0.8%)
Silty clay or sandy silt	49-80 (69)	–	0.16-0.24 (0.21)	3.4N-5.3N	–	–
Silty sand with some gravel	114-127 (121)	–	0.26-0.27 (0.265)	2.9N-3N	–	–
Sandy gravel (GM/GW)	149-188 (169)	–	0.28-0.38 (0.33)	1.6N-2.4N* (1.88N < 100)	> 30	1.7% < $z\,/\,D$

Note: * D: diameter of shafts; z : displacement

REFERENCES

Fellenius, B. H. (2001). "From strain measurements to load in an instrumented pile." *Geotechnical News Magazine*, **19**(1), 35–38.

Lin, S. S., Lin, T., and Chang, L. T. (2000). " A case study for drilled shafts base mud treatment." *New Technological and Design Developments in Deep Foundations*, GSP No. 100, ASCE, 46–58.

O'Neill, M. W. and Reese, L. C. (1999). "Drilled shafts: construction procedures and design methods publication no. FHWA-IF- 99-025." Department of Transportation, Washington D.C., U.S.A.

Rollins, K. M., Clayton, R. T., Mikesell, R. C., and Blaise, B. C. (2005). "Drilled shaft side friction in gravelly soils." *Journal of Geotechnical and Geoenvironmental Engineering*, ASCE, **131**(8), 987–1003.

Stas, C. V. and Kulhawy, F. H. (1984). "Critical evaluation of design methods for foundations under axial uplift and compression loading." Report El-3771, Electric Power Research Institute, Palo Alto, California, U.S.A.

Woo, S. M. (2001). "Design and construction problem of large diameter long piles based on pile load test results." *Proceedings of Pile Talk Symposium*, Taipei, Taiwan, B1–B37.